IEEE/CSC & ESAS European Superconductivity News Forum (ESNF), No. 14, October 2010
The published version of this manuscript appeared in *IEEE Transactions on Applied Superconductivity* **21**, Issue 3, 3251 - 3256 (2011)

Dynamic Resistance of YBCO-Coated Conductors in Applied AC Fields with DC Transport Currents and DC Background Fields

Robert C. Duckworth, Yifei F. Zhang, Tam Ha, and Michael J. Gouge

***Abstract*— In order to predict heat loads in future saturable-core fault-current-limiting devices due to ac fringing fields, dynamic resistance in YBCO-coated conductors was measured at 77 K in peak ac fields up to 25 mT at 60 Hz and in dc fields up to 1 T. With the sample orientation set such that the conductor face was either parallel or perpendicular to the ac and dc applied fields, the dynamic resistance was measured at different fractions of the critical current to determine the relationship between the dc transport current and the applied fields. With respect to field orientation, the dynamic resistance for ac fields that were perpendicular to the conductor face was significantly higher than when the ac fields were parallel to the conductor face. It was also observed that the dynamic resistance: 1) increased with increasing fraction of the dc transport current to the critical current, 2) was proportional to the inverse of the critical current, and 3) demonstrated a linear dependence with the applied ac field once a threshold field was exceeded. This functional behavior was consistent with a critical state model for the dynamic resistance, but discrepancies in absolute value of the dynamic resistance suggested that further theoretical development is needed.**

***Index Terms*— Loss Measurement, Fault Current Limiters, Dynamic Resistance**

I. INTRODUCTION

FAULT current limiters (FCLs) represent a superconducting technology that can provide protection to devices and subsystems within the electric grid. This protection has taken on added importance from the growth of fault current due to the addition of distributed generating capacity, which has pushed fault currents toward levels that are beyond the limits of conventional breaker technology. For most FCL configurations, devices are installed with the superconductor in direct contact to the electric grid and limit the fault through the generation of voltage due to the rapid transition from the superconducting state to the normal resistive state. The non-linear transition is defined by the n-value of the superconductor with n-values between 25-40 desirable for resistive FCL devices. Because of this requirement, $YBa_2Cu_3O_x$ (YBCO) coated conductors [1–4] or $Bi_2Sr_2Ca_1Cu_2O_{7-\delta}$ (BSCCO) cylindrical elements [5–7] are utilized in these types of FCLs. The challenge that these configurations face is balancing the heat generation into the liquid nitrogen environment during the fault against the ability to maintain or recover operation under voltage on the order of seconds and allow for the reconnection to electric grid [8].

One alternative FCL design that is being pursued is the iron-core-saturated FCL, which has been studied by Zenergy [9], Innopower [10], and Korea [11]. This concept uses the superconductor in an isolated, low-voltage dc bias coil to generate a high dc field to saturate an iron core that is linked magnetically to a series of conventional copper phase windings, which are connected to the electric grid. This design eliminates the high-voltage requirement on the superconductor in the cryogenic environment. The fault currents in these copper windings are limited through the impedance that is added by the saturated iron core. The feasibility of this concept has been demonstrated at distribution level voltages (13.8 kV) by Zenergy in the Southern California Edison "grid of the future" and is currently being scaled up for implementation at transmission level voltages (138 kV). With respect to the usage of the superconductor, this FCL configuration isolates the superconductor from direct contact to ac currents and utilizes the superconductor's ability to carry current at operating temperatures that can range from 30 K to 77 K and at dc fields approaching 2 T instead of its rapid, non-linear transition to the normal state. While this configuration reduces the ac loss in the superconductors since it is not carrying ac currents directly, ac loss is generated in the dc coil from the fringing fields that are generated by the conventional windings and iron core. While the amount of ac loss per unit length is generally smaller than the ac loss per unit length in resistive FCLs, the ac loss that is generated due to the interaction between dc currents and ac fields can become significant given that the amount of tape in dc bias coils can range from hundreds of meters to tens of kilometers.

Work on the measurement of ac loss in a superconductor from the interaction between an applied ac field and a dc transport current has focused on connecting geometry and tape performance to ac loss. In general it has been shown the ac loss from this interaction, often referred to as dynamic resistance, depends linearly with frequency and occurs once a given threshold field, $B_{ac,th,}$, is exceeded [12–17]. In BSCCO tapes, Oomen [14] found that the dynamic resistance was

Manuscript received 1 August 2010. Research sponsored by the U.S. Department of Energy, Office of Electricity Delivery and Energy Reliability, Advanced Cables and Conductors, under contract DE-AC05-00OR22725 with Oak Ridge National Laboratory, managed and operated by UT-Battelle, LLC.

R. C. Duckworth, Y. F. Zhang, T. Ha, and M.J. Gouge are with the Applied Superconductivity Group at Oak Ridge National Laboratory, Oak Ridge, TN 37831-6305 (phone: 865-574-2735; fax: 865-576-7770; e-mail: duckworthrc@ornl.gov).

influenced by the dependence of the critical current density with respect to the applied ac field. The tape geometry in BSCCO tapes also influenced the magnitude of the dynamic resistance, with the ratio of the dynamic resistance in perpendicular field to the dynamic resistance in parallel field matching the ratio of the tape width to the tape thickness [15]. Ciszek [16–17] investigated dynamic resistance with respect to YBCO-coated conductors in perpendicular ac fields with dc transport currents and found the dynamic resistance approached 0.3 mΩ/m and an ac loss at 60 Hz near 0.06 W/m at 10 mT of applied ac field.

The purpose of the work presented here is to determine the impact of dc fields up to 1.0 T, ac fields up to 20 mT, YBCO conductor architecture, and tape performance on dynamic resistance. This was accomplished with the development of a new test facility to obtain the functional dependence of the dynamic resistance of YBCO-coated conductors with respect to dc transport current, dc field, ac fields, and orientation of the the applied fields to the tape face. Results will be compared to measurements that were carried out on a multifilamentary BSCCO tape and to a critical state model for dynamic resistance to confirm the role of tape geometry and composition. While this type of iron-core-saturated FCL device operates at lower temperatures between 20 K and 50 K, initial characterization of YBCO-coated conductors at 77 K will provide the functional dependence of the dynamic resistance that will be useful for system designers.

II. Theoretical Background

The phenomenon of dynamic resistance was initially discovered during analysis of field decay in persistent low-temperature superconducting (LTS) magnets. While operating at constant dc current, resistance was measured from the presence of fringing ac fields and this resistance generated heat that caused an increase in temperature and a decay in available dc current in the magnet, and its eventual quench. While Ogasawara [18] developed a critical state model for the dynamic resistance in a round wire to explain this phenomenon, Oomen [14] developed an expression of dynamic resistance in high-aspect-ratio tape geometries using this model as a starting point. With a dc current, I_t, and an applied ac field parallel to the tape face, B_{ac}, as shown in Fig. 1, the dynamic resistance within the superconducting tape with thickness d, length L, and width $2a$ can be written

$$R_{dyn}/L = 4af\left(B_{ac} - B_{ac,th}\right)/I_c \ , \qquad (1)$$

where the threshold field, $B_{ac,th}$, above which this resistance appears can be expressed as

$$B_{ac,th} = \mu_o I_c(1-i)/2d \ , \qquad (2)$$

where $i = I_t/I_c$. Below this threshold field, R_{dyn}/L is zero. For the purposes of comparing our results to these expressions, the critical current, I_c, was its value at a given applied dc field, B_{dc}, which was applied in the same direction as B_{ac}. When the field was applied perpendicular to the sample, the thickness and width are interchanged in (1) and (2) based on the supporting results for BSCCO tapes that is given in [13,15]. This model was used to interpret the experimental results and determine whether the critical state model is suitable for YBCO-coated conductors.

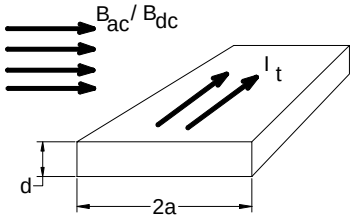

Fig. 1. Schematic of tape geometry with respect to applied ac field as utilized in theoretical treatment of dynamic resistance by Oomen.

III. Experimental Setup and Measurment

In order to perform the measurements with a specified dc transport current and dc field with a background ac field, integration of existing equipment was carried out to allow for the measurements of dynamic resistance at 77 K and 60 Hz. The background dc field was provided by a LTS solenoid magnet with a maximum central field of 6 T and a central bore of 17.5 cm. A liquid nitrogen dewar was positioned in the central bore, and a resistive solenoid magnet with a peak field of 100 mT was inserted into the dewar to provide the ac field. For this configuration, which is pictured in Fig. 2, the position of the resistive solenoid magnet was adjusted until the fields at the center of the magnets were aligned.

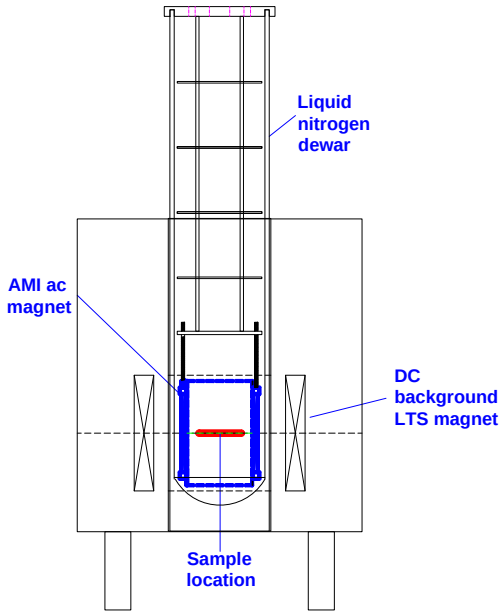

Fig. 2. Schematic for dynamic resistance measurement of YBCO coated conductor as a function of dc transport current up to 90% of the sample critical current, dc background fields up to 1 T, and ac fields up to 25 mT.

The sample was secured at the center of the ac magnet and voltage taps were attached in the S-shaped pattern as shown in Fig. 3 as recommended in [19]. This voltage tap arrangements was utilized with an ac bucking coil and a Keithley 2182 nanovoltmeter to minimize the contribution of inductive pickup and noise generated by the ac field during the measurement and measured the voltage that was generated from the transport current and applied fields.

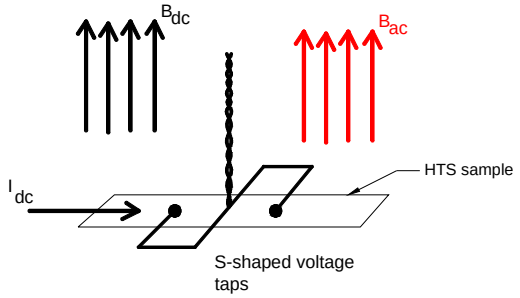

Fig. 3. Layout of voltage taps that were connected to YBCO coated conductor along with orientation of applied dc and ac background fields to tape face for a perpendicular field case.

After the sample orientation was fixed with the tape face either parallel or perpendicular to the ac/dc fields, the sample was cooled down to 77 K, the dc background field was set, and the dc current increased until a 1 μV/cm voltage was reached to define the critical current. After setting the dc current to a particular fraction of the critical current, ac current was applied to the resistive magnet and the voltage across the sample was measured from the corresponding ac field. This ac field was held constant for 5 to 10 seconds to average the voltage and limit the heat that was generated from the interaction between the resistive magnet and the dc background field. The ac current to the resistive magnet was varied to map out peak ac fields from 0 to 25 mT. The frequency of the applied ac field was 60 Hz. After the measurement was completed for the specified ac field range, the dc current was then set to another percentage of the dc critical current and the ac field applied again over the same range. Once the voltages were measured for different percentages of dc current, the dc field was set to another value, the critical current measured at this dc field, and the entire process was repeated over different dc fields up to 1 T.

IV. Results and Analysis

Both YBCO and BSCCO high-temperature superconducting (HTS) tapes were characterized as a function of ac/dc fields and dc currents. Characterization of both types of HTS tape was done to determine the effects of geometry and sample composition on dynamic resistance. Table I summarizes the properties of the HTS conductors. The dependence of the critical current with respect to the dc field both perpendicular and parallel to the tape face is given in Fig. 4.

A. Dynamic Resistance Characterization (YBCO-1)

The dynamic resistance as a function of applied ac/dc fields that were perpendicular to the tape face is shown in Figs. 5 and 6 for YBCO-1 at different fractions of total current to critical current and at different applied dc fields. From each figure, once the threshold field is exceeded, the dynamic resistance displays a linear dependence with respect to the applied ac field. It is clear that the observed increase in dynamic resistance coincided with a drop in critical current. These functional dependencies of the dynamic resistance with respect to threshold fields and critical current are consistent with the expressions in (1) and (2).

TABLE I. Specifications of BSCCO and YBCO tapes

Parameters	BSCCO	YBCO-1	YBCO-2
Width (*2a*)	4 mm[a]	4 mm	4 mm[a]
Thickness of superconductor	0.2 mm	1 μm	1 μm
Critical current at 77 K	120 A	123 A	97 A
Stabilization	Stainless steel laminated	Copper plated	Brass laminated
Total stabilization thickness	100 μm	40 μm	200 μm
Manufacturer	AMSC	SP	AMSC

[a]Width for YBCO-2 refers the width of the HTS insert tape and not the overall tape width, which is nominally 4.4 mm.

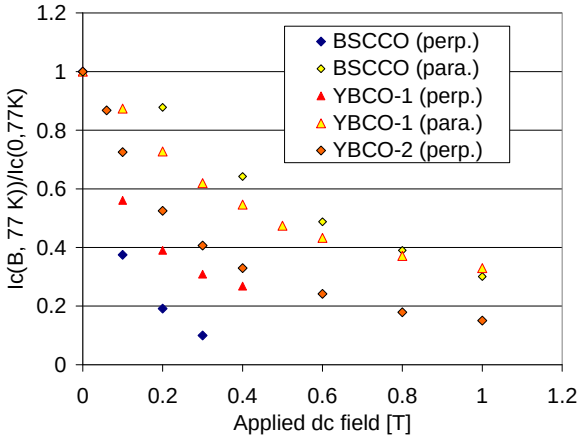

Fig. 4. Critical current at 77 K and both perpendicular and parallel dc fields for BSCCO, YBCO-1, and YBCO-2 as specified in Table I.

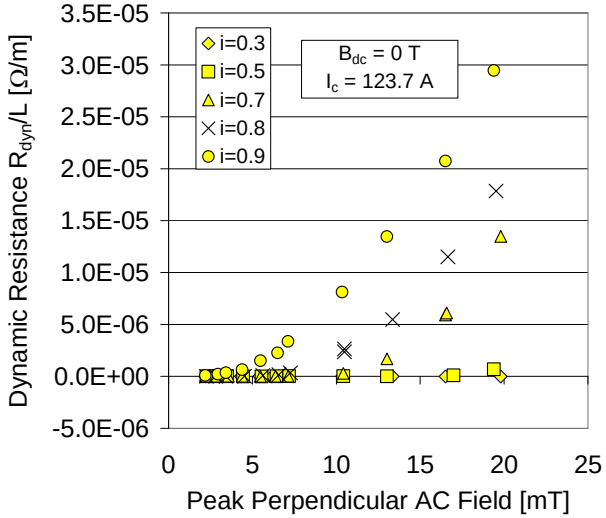

Fig. 5. Dynamic resistance at 77 K and 60 Hz as different fractions of current as a function of applied ac field perpendicular to the tape in YBCO-1 (SP) in self field.

To determine whether the dynamic resistance of YBCO-1 can be explained by the critical state model as given by (1) and (2), the threshold field was calculated from (2) by

assuming the critical currents of Fig. 4 at different fractions of the critical current, *i*. These calculations were compared to the threshold fields that were found from the experimental data by finding the ac field when R_{dyn}/L approaches zero. From Fig. 7, the experimental threshold field was approximately a factor of two to three higher than the threshold field predicted by (2).

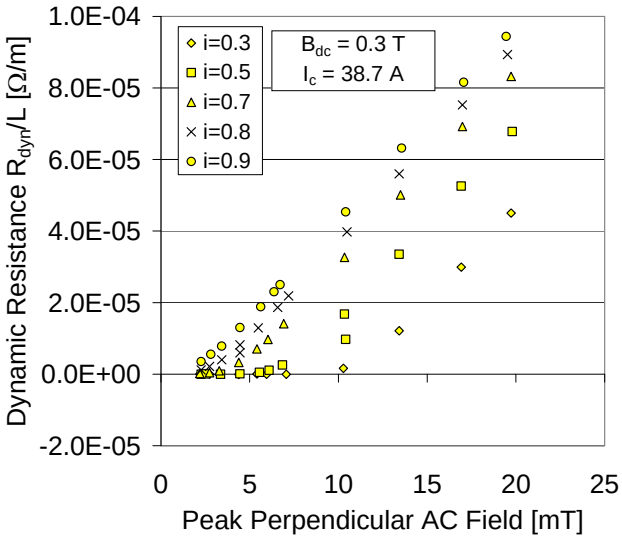

Fig. 6. Dynamic resistance at 77 K and 60 Hz as different fractions of current as a function of applied ac field perpendicular to the tape in YBCO-1 (SP) in background dc field of 0.3 T.

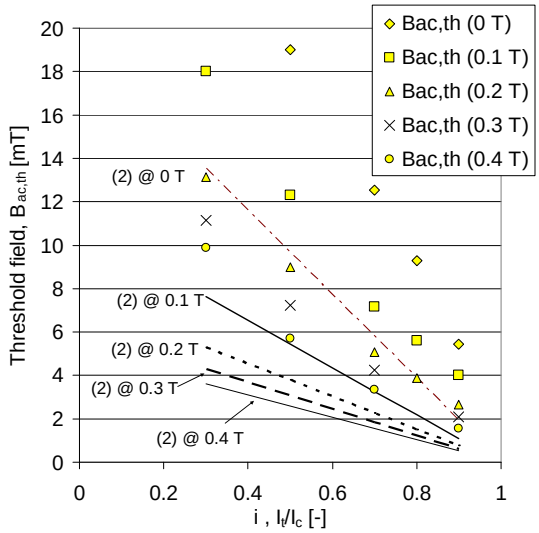

Fig. 7. Comparison of threshold field as calculated for YBCO-1 by (2) and the threshold fields found from the analysis of the experimental data.

Measurements were also carried out with the ac and dc fields parallel to the tape face with dc fields up to 1.0 T. However, no dynamic resistance was observed over the ac field range up to 20 mT. The absence of dynamic resistance is consistent with expected threshold fields from (2) for YBCO-1 and YBCO-2 since they both have a superconductor thickness on the order of 1 µm. Using the parameters shown in Table I and Fig. 4 for the critical current performance at 1 T, the threshold field for YBCO-1 should be 2.0 T, which is 100 times larger than the applied ac field in this experiment. In fact, the critical current of a YBCO-coated conductor would have to drop to 0.5 A in order for the threshold field to be small enough to be observed at the 20 mT level.

B. Dynamic Resistance Characterization (YBCO-2)

The influence of the template architecture on functional dependence of the dynamic resistance was established through the measurement of YBCO-2 as a function of applied ac/dc fields that were perpendicular to the tape face, which is shown in Figs. 8 and 9 at different fractions of total current to critical current at a fixed, applied dc field. As with the results for YBCO-1, once the threshold field is exceeded, the dynamic resistance displayed the linear dependence with respect to the applied ac field as given by (1) and the observed increase in dynamic resistance coincided drop in critical current. As was done for YBCO-1, the threshold fields for YBCO-2 were obtained from the experimental data and compared to the predicted threshold fields given by (2) in Fig. 10. The difference between the experimental values and the theory was again a factor of two to three.

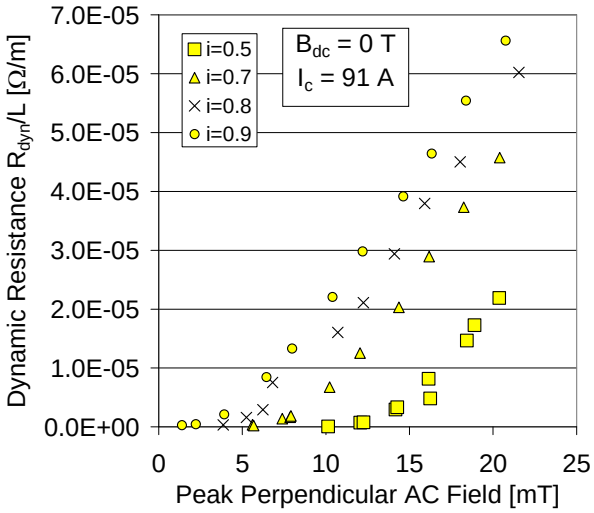

Fig. 8. Dynamic resistance at 77 K and 60 Hz as different fractions of current as a function of applied ac field perpendicular to the tape in YBCO-2 (AMSC) in self field.

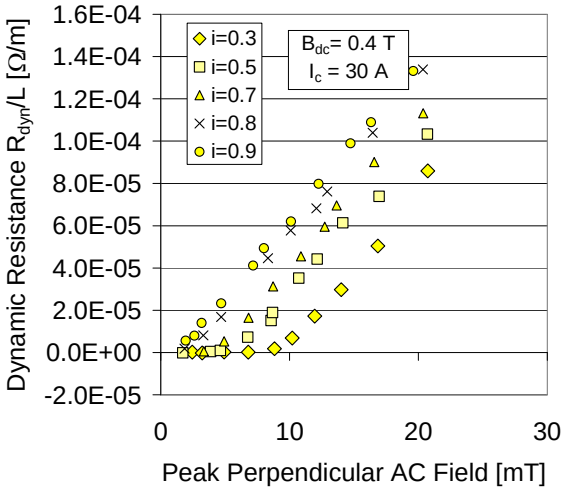

Fig. 9. Dynamic resistance at 77 K and 60 Hz as different fractions of current as a function of applied ac field perpendicular to the tape in YBCO-2 (AMSC) in background dc field of 0.4 T.

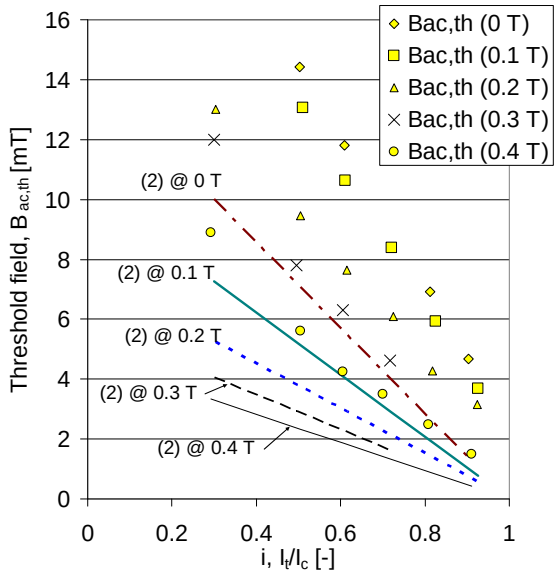

Fig. 10. Comparison of threshold field as calculated for YBCO-2 by (2) and the threshold fields found from the analysis of the experimental data.

The reason for discrepancy in the threshold fields is likely due to the fact that the assumptions for (1) and (2) are not sufficient for YBCO-coated conductors. With respect to geometry, (1) and (2) are expressions for the dynamic resistance with the fields parallel to the tape face, while the results shown in Figs. 5 and 6 and Figs. 8 and 9 have the ac/dc fields perpendicular to the tape face. While the interchange of the dimensions of thickness and width in (1) and (2) for BSCCO was supported by the experimental findings of Ciszek [13,15], this does not appear to be case for the YBCO-coated conductor.

Another assumption in question is the use of the critical state model for the current density that is used to derive (1) and (2). In an investigation done by Oomen [14] for BSCCO wires, it was found that while the critical state provided a good starting point, better agreement between theory and experiment was found by assuming a field-dependent current density. Since the field-dependent current density in YBCO still has variation from sample to sample, further theoretical development or finite-element simulation is required to ascertain the influence of geometry completely. However, it should be emphasized that while there are differences in the ability for (1) and (2) to predict the absolute value of the dynamic resistance for YBCO precisely, the functional dependence of the dynamic resistance with respect to applied field, the ratio of current to critical current, and the absolute value of the critical current from these results are consistent with (1) and (2).

Finally, the similarities with respect to the dynamic resistances and the behavior with respect to threshold field for YBCO-1 and YBCO-2 would indicate that the template architecture does not influence the dynamic resistance significantly at these conditions. This indicates that modification to (1) and (2) would not require the template to be taken into account.

C. Comparison of Dynamic Resistance in YBCO-Coated Conductor to BSCCO Wires

The dynamic resistance of YBCO-coated conductors was compared to the dynamic resistance of BSCCO at 77K and 60 Hz. In order to make a meaningful comparison with respect to the two conductors, the percentage of critical current was fixed at 70% and the data chosen for each conductor was done such that the critical currents for each sample were identical. Figs. 11 and 12 show the dynamic resistance as a function of the applied perpendicular ac field for two cases with the critical current of the tapes at approximately 47 A and 22 A, respectively. It is clear that there is a distinct difference between the dynamic resistances of YBCO to BSCCO under these conditions. If the thicknesses of the superconductor are used in (1) and (2), the dynamic resistance in BSCCO should be greater than YBCO given the difference in the superconductor thickness. This finding when combined with the differences that were found in the threshold fields of YBCO-1 and YBCO-2 in Figs. 7 and 10, respectively, would support that additional theoretical development and finite-element modeling is required.

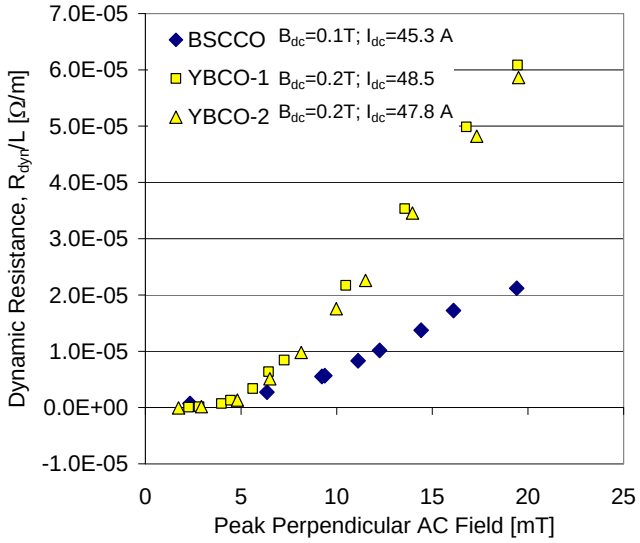

Fig. 11. Dynamic resistance at 77 K and 60 Hz at a 70% fraction of the dc current to the critical current and at similar critical currents (45-48 A) for the three HTS conductors, BSCCO, YBCO-1, and YBCO-2.

V. Conclusions and Future Directions

The dynamic resistance was characterized as a function of dc field, dc transport current, and ac field for YBCO-coated conductors at 77 K and 60 Hz and compared to the dynamic resistance in BSCCO wires as well as existing theoretical expressions for the dynamic resistance. From the comparisons that were done with respect to these results, the functional dependence of the dynamic resistance with respect to the ac field, critical current, and the fraction of the dc current to the critical current was consistent with that predicted by theory. However, there were observable differences in the absolute value of the dynamic resistance as well as the increase in the dynamic resistance of YBCO-coated conductors when compared to BSCCO wires that would suggest that further refinement of existing theories is required. Future work will include revising the theoretical expression of dynamic

resistance with respect to YBCO-coated conductors, further measurements at temperatures between 30 K and 77 K to determine whether the findings at 77 K are consistent at higher dc fields and critical currents.

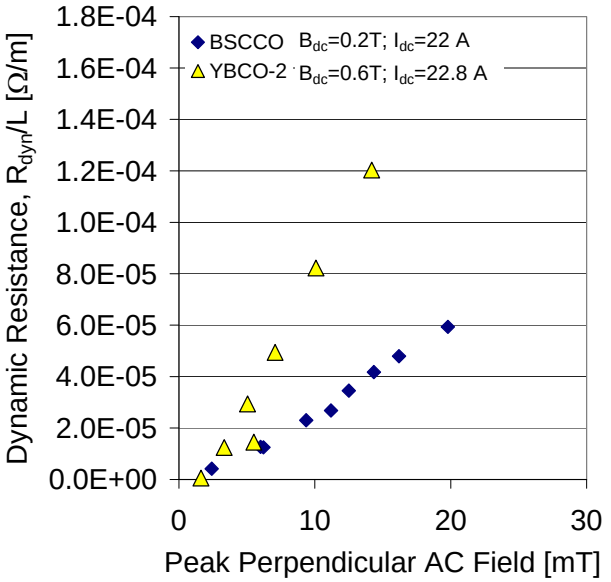

Fig. 12. Dynamic resistance at 77 K and 60 Hz at a 70% fraction of the dc current to the critical current and at similar critical currents (22-23 A) for the two of HTS conductors, BSCCO and YBCO-2.

ACKNOWLEDGMENT

The authors would like to thank Frank Darmann and his team at Zenergy, Inc., for their technical insights and discussions during the course of this work.

REFERENCES

[1] A.P. Malozemoff, S. Fleshler, M. Rupich, C. Thieme, X. Li, W. Zhang, A. Otto, J. Maguire, D. Folts, J. Yuan, H.-P. Kraemar, W. Schmidt, M. Wohlfart, and H.-W. Neumueller, "Progress in high temperature superconductor coated conductors and their applications," *Supercond. Sci. Tech.*, vol. 21, p. 034005, 2008.

[2] J. Maguire, D. Folts, J. Yuan, D. Lindsay, D. Knoll, S. Bratt, Z. Wolff, and S. Kurtz, "Development and demonstration of a fault current limiting HTS cable to be installed in the Con Edison grid," *IEEE Trans. Appl. Supercond.*, vol. 19, pp. 1740–1743, 2009.

[3] T. Yazawa, K. Koyonagi, M. Takahashi, M. Ono, M. Sakai, K. Toba, H. Takigami, M. Urata, Y. Iijima, T. Saitoh, N. Amemiya, and Y. Shiohara, "Design and Experimental results of three-phase superconducting fault current limiter using highly-resistive YBCO tapes," *IEEE Trans. Appl. Supercond.*, vol. 19, pp. 1956–1959, 2009.

[4] H. Kang, C. Lee, K. Nam, Y.S. Yoon, H.-M. Chang, T.K. Ko, B.-Y. Soek, "Development of a 13.2 kV/620A (8.3MVA) high temperature superconducting fault current limiter," *IEEE Trans. Appl. Supercond.*, vol.18, pp. 628–631, 2008.

[5] J. Sim, H.G. Lee, S.-W. Yim, I. Choi, H.-R. Kim, O.-B. Hyun, H.M. Kim, K.B. Park, B.W. Lee, I.S. Oh, F. Breuer, and J. Bock, "Fault current limitation characteristics of Bi-2122 bulk coil with different types of shunt coils," *IEEE Trans. Appl. Supercond.*, vol. 17, pp. 1879–1882, 2007

[6] J. Bock, F. Breuer, H. Walter, M. Noe, R. Kreutz, M. Kleimaier, K.-H. Weck, and S. Eischner, "Development and successful testing of MCP BSCCO-2212 components for a 10 MVA superconducting fault current limiter," *Supercond. Sci. Tech.*, vol. 17, pp. S122–S126, 2004.

[7] M. Chen, W. Paul, M. Lakner, L. Donzel, M. Holdis, P. Unternauehrer, R. Weder, and M. Mendik, "6.4 MVA resistive fault current limiter based on Bi-2212 superconductor," *Physica C*, vols. 372–376, pp. 1657–1563, 2002.

[8] W. Schmidt, B. Gamble, H.-P. Kraemer, D. Madura, A. Otto, and W. Romanosky, "Design and test of current limiting modules using YBCO-coated conductors," *Supercond. Sci. Tech.*, vol. 23, p. 014024, 2010.

[9] F. Moriconi, N. Koshnick, F. de la Rosa, and A. Singh, "Modeling and test validation of a 15 kV 24 MVA superconducting fault current limiter," *2010 IEEE/PES Transmission and Distribution Conference and Exposition*, p. 6, 2010.

[10] Y. Xin, W. Gong, X. Niu, Z. Chao, J. Zhang, B. Tian, Y. Wang, H. Hong, X.Y. Niu, Q. Li, and L.F. Zhang, "Development of saturated iron core HTS fault current limiters," *IEEE Trans. Appl. Supercond.*, vol. 17, pp. 1760-1763, 2007

[11] S.-H. Lim, J.-F. Moon, and J.-C. Kim, "Improvement on current limiting characteristics of a flux-lock type SFCL using E-I core," *IEEE Trans. Appl. Supercond.*, vol. 19, pp. 1904–1907, 2009

[12] M.P. Oomen, J. Rieger, M. Leghissa, and H.H.J. ten Kate, "Magnetic ac loss in multifilamentary Bi-2223/Ag tapes," *Physica C*, vol. 290, pp. 281–290, 1997.

[13] M. Ciszek, B.A. Glowacki, A.M. Campbell, S.P. Ashworth, W.Y. Liang, P. Haldar, and V. Selvamanickam, "Influence of external magnetic field and its orientation on transport AC losses in Bi-2223 and Tl-1223 silver sheathed tapes," *IEEE Trans. Appl. Supercond.*, vol. 7, pp. 314–317, 1997.

[14] M.P. Oomen, J. Rieger, M. Leghissa, B. ten Haken, and H.H.J. ten Kate, "Dynamic resistance in a slab-like superconductor with Jc(B) dependence," *Supercond. Sci. Tech*, vol. 12, pp. 382–387, 1999.

[15] M. Ciszek, H.G. Knoopers, J.J. Rabbers, B. ten Haken, and H.H.J. ten Kate, "Angular dependence of the dynamic resistance and its relation to the AC transport current loss in Bi-2223/Ag tape superconductors," *Supercond. Sci. Tech.*, vol. 15, pp. 1275–1280, 2002.

[16] M. Ciszek, O. Tsukamoto, J. Ogawa, and D. Miyagi, "Energy losses in YBCO-123coated conductors carrying transport current in perpendicular external magnetic field," *Advances in Cryogenic Engineering – ICMC*, vol. 48, pp. 608–613, 2002.

[17] M. Ciszek, O. Tsukamoto, J. Ogawa, and M. Shiokawa, "Energy loss in YBCO-123 coated conductor due to AC/DC transport current and AC external perpendicular magnetic field," *Physica C*, vol. 387, pp. 230–233, 2003.

[18] T. Ogasawara, K. Yasukochi, S. Nose, and H. Seikizawa, "Effective resistance of current-carrying superconducting wire in oscillating fields 1: Single core composite conductor," *Cryogenics*, vol. 16, pp. 33–38, 1976.

[19] J.J. Rabbers, B. ten Haken, and H.H.J. ten Kate, "Advanced ac loss measurement methods for high-temperature superconducting tapes," *Rev. Sci. Inst.*, vol. 72, pp. 2365–2373, 2001.